Electronic Supplementary Material (ESI) for New Journal of Chemistry.

Electronic Supplementary Information

Exploring flowery MnO_2/Ag nanocomposites as an efficient solar light driven photocatalyst

Arnab Samanta,[a] Samir Kumar Pal[a,b] and Subhra Jana[a,b]*

[a]Department of Chemical, Biological & Macro-Molecular Sciences, [b]Technical Research Centre, S. N. Bose National Centre for Basic Sciences, Block - JD, Sector-III, Salt Lake, Kolkata -700 106, India.

E-mail: subhra.jana@bose.res.in, subhra.jana@gmail.com

Materials

All chemicals were used as received. Potassium permanganate ($KMnO_4$), silver nitrate($AgNO_3$), toluene, ethanol, sodium azide and hydrogen peroxide were received from Merck. Sodium hydroxide (NaOH), methylene blue (MB) and eosin yellow (EY) were obtained from Sisco Research Laboratory (SRL), India. tert-Butanol (t-BA) and triethanolamine (TEA) were purchased from Spectrochem India. Halloysite nanotubes (HNTs) were received from Sigma-Aldrich and (3-aminopropyl)triethoxysilane was purchased from Alfa Aesar.

Characterization

The surface morphology of prepared nanocomposites was observed via a field emission scanning electron microscopy (FESEM: FEI QUANTA FEG 250) and transmission electron microscopy (TEM: FEI TECNAI G2 F20-ST) after drop casting a drop of solution on a silicon wafer and a carbon coated copper grid respectively. High resolution transmission electron microscopy (HRTEM) and Energy dispersive X-ray spectroscopy (EDS) analyses were performed in the above-mentioned TEM using an accelerating voltage of 200 kV. Powder X-ray diffraction (XRD) patterns were recorded on a RIGAKU MiniFlex II powder diffractometer using Cu Kα radiation with 35 kV beam voltage and 15 mA beam current. Inductively coupled plasma optical emission spectrometry (ICP-OES) analysis was carried out using the PerkinElmer ICP-OES instrument (PerkinElmer, Inc., Shelton, CT, USA). Specific surface area was determined by the BET method using nitrogen adsorption/desorption isotherms at 77 K with 3flex Micromeritics analyzer. X-ray photoelectron spectroscopy (XPS) was carried out using a monochromatized Al Kα (1486.6 eV) as X-ray source (Omicron Nanotechnology instrument). The UV-visible diffuse

reflectance absorption spectrum of the nanocomposites was obtained using the same spectrophotometer (Shimadzu) equipped with a diffuse reflectance accessory.

Surface functionalization of halloysite nanotubes (HNTs)

Organosilane grafted halloysite nanotubes were synthesized according to the following procedure. The grafting reaction was carried out under nitrogen atmosphere using standard air free techniques. A total of 3.0 g of HNTs was taken in a 50 mL three-necked round-bottom flask containing 15.0 mL of toluene. Afterward, the reaction flux was fixed with a rubber septum, condenser, thermocouple adaptor, and additional quartz sheath in which a thermocouple was inserted. The reaction mixture was deaerated for 30 min under nitrogen at room temperature, followed by heated with a heating mantle. Then, 1.5 mL of (3-aminopropyl) triethoxysilane was injected into the reaction flask at 60 °C under stirring condition and refluxed for 20 h. Finally, the as-synthesized product was collected through filtration and washed several times with toluene and ethanol, respectively. The obtained product was dried at 100 °C overnight under vacuum.

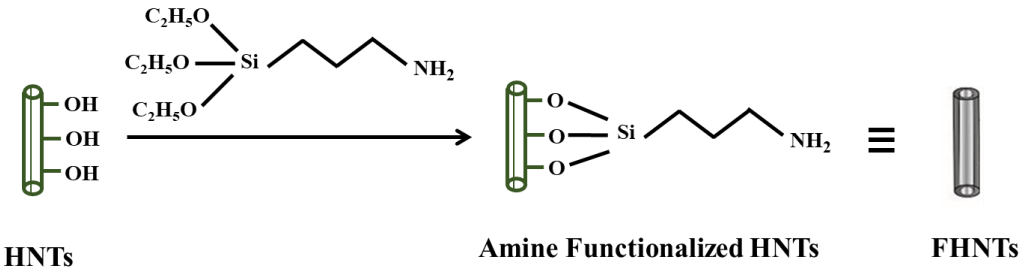

Fig. S1 Schematic presentation of the functionalization of the surface of the halloysite nanotubes (HNTs) through grafting of an aminosilane leading to the formation of amine functionalized HNTs (FHNTs).

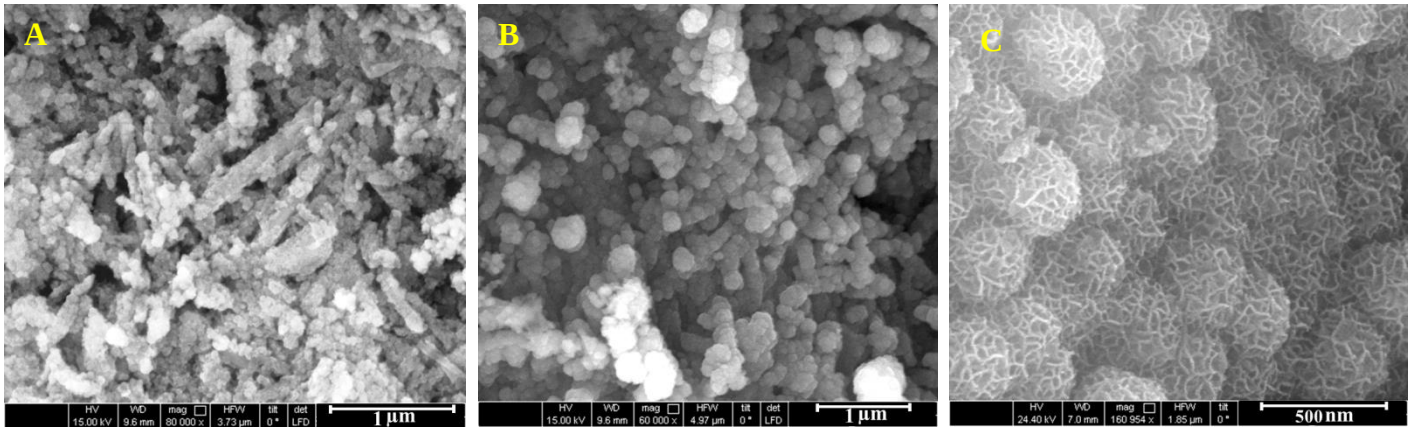

Fig. S2 Time dependent growth of MnO_2 NCs over the surface of FHNTs, clearly indicates the formation of MnO_2 flowery nanostructures. FESEM images of the intermediates during the formation of flower-like MnO_2 NCs at different reaction times, (A) 2 h, (B) 5 h and (C) 10 h.

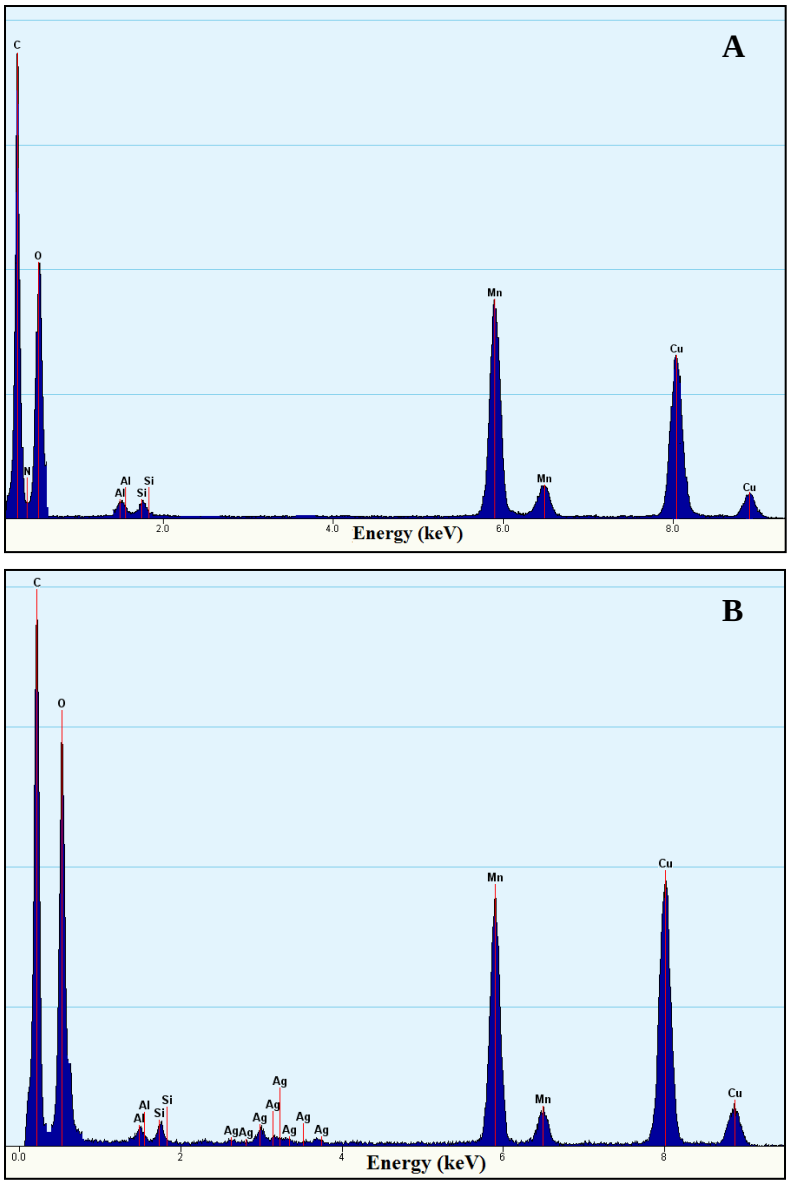

Fig. S3 EDS spectra of (A) MnO_2 and (B) MnO_2/Ag NCs. In EDS spectrum of MnO_2/Ag NCs, new signals are observed for Ag together with the previously observed peaks for pristine MnO_2.

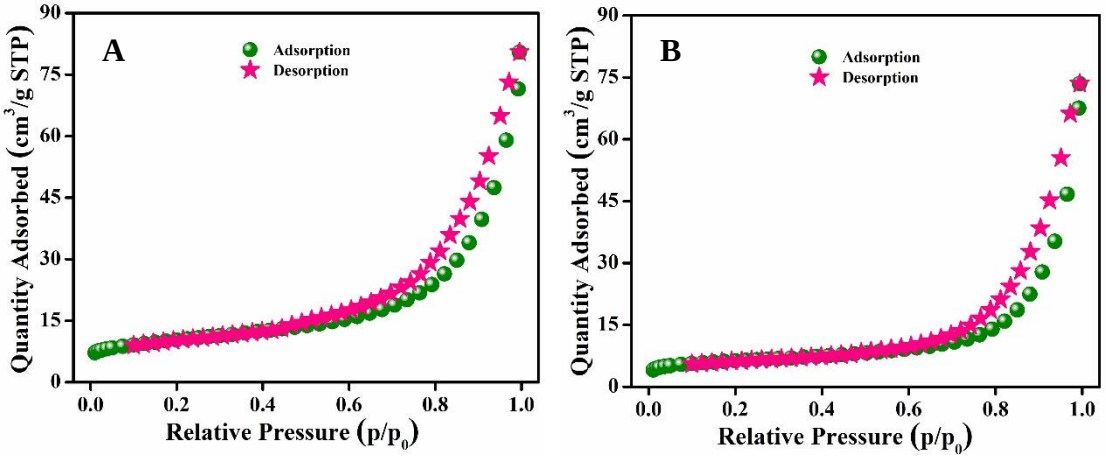

Fig. S4 The nitrogen adsorption-desorption isotherms of (A) MnO_2 and (B) MnO_2/Ag NCs.

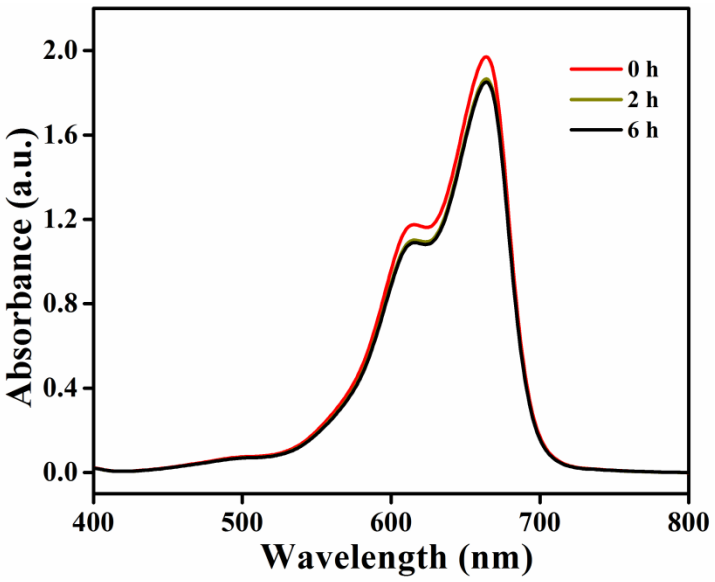

Fig S5. UV-Visible absorption spectra of MB during the adsorption-desorption equilibrium study by MnO_2/Ag NCs as a function of time. An adsorption of ~7% of MB was observed during the adsorption-desorption equilibration under dark condition.

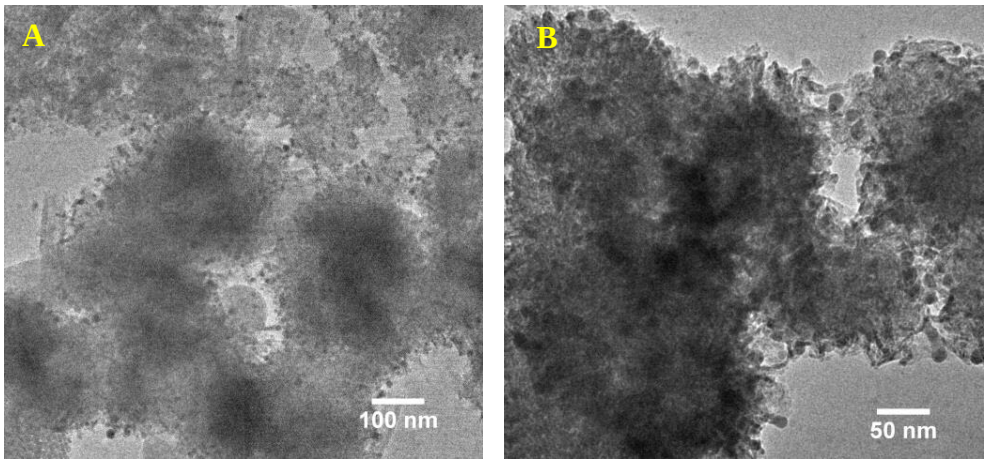

Fig. S6 TEM micrographs of MnO_2/Ag NCs after photocatalysis.

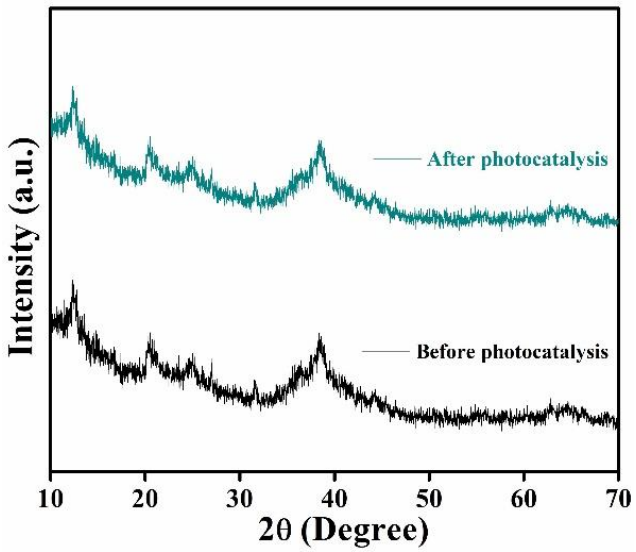

Fig. S7 XRD patterns of MnO_2/Ag NCs before and after photocatalysis.

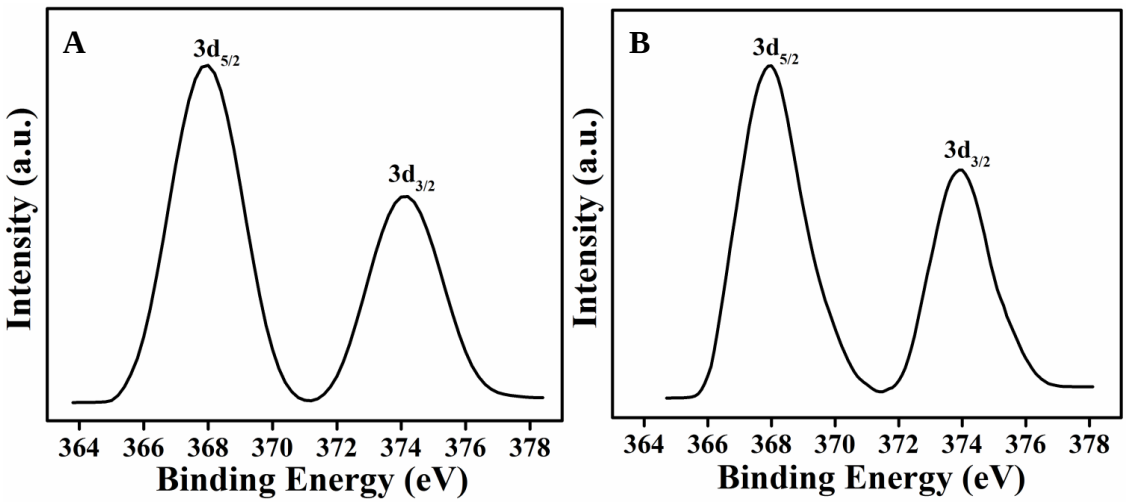

Fig. S8 XPS spectra of Ag 3d in MnO_2/Ag (A) before and (B) after photocatalytic experiment.

Table S1 Comparison of the degradation efficiency of MnO_2/Ag NCs with the other reported MnO_2 based catalysts for the degradation of methylene blue.

Catalysts	Irradiation Time (min)	Degradation Efficiency (%)	References
δ-MnO_2/ montmorillonite	700	92	1
Cu doped MnO_2@diatomite	240	96.2	2
Fe_3O_4@polydopamine-MnO_2	240	97.36	3
MnO_2/Fe_3O_4	180	98.2	4
Fe_3O_4/SiO_2/MnO_2/BiOBr-Bi	150	95.23	5
Polyaniline-modified MnO_2 composite	120	94	6
MnO_2/TiO_2 nanocomposite	120	90	7
PANI-rGO-MnO_2	120	90	8
β-MnO_2	120	90.2	9
Fe/M-MnO_2	120	94.8	10
MnO_2/CH-FP	90	95.6	11
MPS-(MnO_2) nanocomposite	90	89.4	12
MnO_2/$BiVO_4$/GNP	60	76	13
Mn_3O_4-MnO_2 composite	60	93.5	14
MnO_2 NCs	**70**	**95.7**	**Present Work**
MnO_2/Ag NCs	**40**	**96.8**	**Present Work**

References:

1 M. X. Zhu, Z. Wang, S. H. Xu and T. Li, *J. Hazard. Mater.*, 2010, **181**, 57-64.

2 Y. Xiao, W. Huo, S. Yin, D. Jiang, Y. Zhang, Z. Zhang, X. Liu, F. Dong, J. Wang, G. Li and X. Hu, *J. Colloid Interface Sci.*, 2019, **556**, 466-475.

3 X. Pan, S. Cheng, T. Su, G. Zuo, W. Zhao, X. Qi, W. Wei and W. Dong, *Colloids Surf. B Biointerfaces*, 2019, **181**, 226-233.

4 L. Zhang, J. Lian, L. Wu, Z. Duan, J. Jiang and L. Zhao, *Langmuir*, 2014, **30**, 7006-7013.

5 M. Ma, Y. Yang, Y. Chen, Y. Ma, P. Lyu, A. Cui, W. Huang, Z. Zhang, Y. Li, and F. Si, *J. Alloys Compd.*, 2021, **861**, 158256.

6 H. Xu, J. Zhang, Y. Chen, H. Lu, J. Zhuang and J. Li, *Mater. Lett.*, 2014, **117**, 21-23.

7 M. Xue, L. Huang, J. Q. Wang, Y. Wang, L. Gao, J. H. Zhu and Z. G. Zou, *Nanotechnology*, 2008, **19**, 185604.

8 Y. Park, A. Numan, N. Ponomarev, J. Iqbal and M. Khalid, *J. Environ. Chem. Eng.*, 2021, **9**, 106006.

9 G. Cheng, L. Yu, T. Lin, R. Yang, M. Sun, B. Lan, L. Yang and F. Deng, *J. Solid State Chem.*, 2014, **217**, 57-63.

10 R. Huang, Y. Liu, Z. Chen, D. Pan, Z. Li, M. Wu, C. H. Shek, C. L. Wu and J. K. Lai, *ACS Appl. Mater. Interfaces*, 2015, **7**, 3949-3959.

11 J. Yang, Z. Ao, H. Wu and S. Zhang, *Chemosphere*, 2021, **268**, 128835.

12 E. Thenmozhi, M. Harshavardhan, S. Kamala-Kannan and V. Janaki, *Mater. Lett.* 2022, **309**, 131367.

13 K. Trzciński, M. Szkoda, M. Sawczak, J. Karczewski and A. Lisowska-Oleksiak, *Appl. Surf. Sci.*, 2016, **385**, 199-208.

14 J. Zhao, J. Nan, Z. Zhao, N. Li, J. Liu and F. Cui, *Appl. Catal. B Environ.*, 2017, **202**, 509-517.